Casimir effect for a semitransparent wedge and an annular piston

Kimball A. Milton[*] and Jef Wagner[†]

*Oklahoma Center for High Energy Physics and Homer L. Dodge Department of Physics and Astronomy, University of Oklahoma,
Norman, Oklahoma 73019-2061, USA*

Klaus Kirsten[‡]

Department of Mathematics, Baylor University, Waco, Texas 76798-7328, USA

We consider the Casimir energy due to a massless scalar field in a geometry of an infinite wedge closed by a Dirichlet circular cylinder, where the wedge is formed by δ-function potentials, so-called semitransparent boundaries. A finite expression for the Casimir energy corresponding to the arc and the presence of both semitransparent potentials is obtained, from which the torque on the sidewalls can be derived. The most interesting part of the calculation is the nontrivial nature of the angular mode functions. Numerical results are obtained which are closely analogous to those recently found for a magnetodielectric wedge, with the same speed of light on both sides of the wedge boundaries. Alternative methods are developed for annular regions with radial semitransparent potentials, based on reduced Green's functions for the angular dependence, which allows calculations using the multiple-scattering formalism. Numerical results corresponding to the torque on the radial plates are likewise computed, which generalize those for the wedge geometry. Generally useful formulas for calculating Casimir energies in separable geometries are derived.

I. INTRODUCTION

The Casimir effect [1], which was originally conceived as the attraction between parallel perfectly conducting plates, may be regarded as due to the fluctuations of the electromagnetic field in the quantum vacuum. In the past six decades, this phenomenon has been generalized to many different types of fields and to a variety of geometries and topologies. Recent reviews of the Casimir effect include Refs. [2–6].

In this paper we will illustrate some new features that arise, for example, in cylindrical geometries in which the cylindrical symmetry is broken. In the past three decades there have been many works on problems possessing cylindrical symmetry, starting with the calculation of the Casimir energy of an infinitely long perfectly conducting cylindrical shell [7]. The more physical but also significantly more involved case of a dielectric cylinder was considered more recently [8–14]. Particularly germane to the present work is the calculation of the Casimir effect for a scalar field interior and exterior to a cylindrical δ-function potential, a so-called semitransparent cylinder [15]; in the weak-coupling limit, both the semitransparent cylinder and the dielectric cylinder have vanishing Casimir energy.

The infinite wedge is closely related to the cylindrical geometry. This problem was first considered in the late seventies [16,17] as part of the still ongoing debate about how to interpret various divergences in quantum field theory with sharp boundaries and whether self-energies of objects have any physical significance. Since then, variations on this idea of the wedge have been treated by several authors [18–22], and reviewed in Ref. [23]. A wedge with a coaxial cylindrical shell was considered by Nesterenko *et al.* [24,25], and the corresponding local stresses were investigated by Saharian and collaborators [26–30]. The interaction of an atom with a wedge was studied in Refs. [31–35]; this geometry is that of the experiment by Sukenik *et al.* carried out more than 15 years ago [36]. Recently, Brevik, Ellingsen, and Milton [37] calculated the Casimir energy of a magnetodielectric cylinder intercut by a perfectly reflecting wedge filled with magnetodielectric material. In all of these studies the assumption was made that the wedge be bounded by perfectly conducting walls.

Although wedges defined by perfect conductors or Dirichlet boundaries break cylindrical symmetry, they do so in an easily understood way. When cylindrical symmetry is present, the azimuthal quantum number ν ranges from $-\infty$ to ∞ by integer steps. With a perfect conductor, which forces the tangential electric field to vanish on the surface, ν takes on values which are related to the opening angle α of the wedge, $\nu = \pi m / \alpha$, where m is an integer. But what if the wedge boundaries are not perfect? Recently, Ellingsen, Brevik, and Milton [38] considered just such a case, where the wedge was defined by the interface between two magnetodielectric media, where the interior sector of the wedge had permittivity ε_1 and permeability μ_1, while the exterior sector had permittivity

[*]milton@nhn.ou.edu
[†]wagner@nhn.ou.edu
[‡]Klaus_Kirsten@baylor.edu

ε_2 and permeability μ_2. The geometry was completed by inserting a perfectly conducting circular cylinder of radius a centered on the wedge axis. To ensure a finite result, as well as separability of the problem, the further assumption was made there that the speed of light in both media was the same: $\varepsilon_1\mu_1 = \varepsilon_2\mu_2$. In this case the azimuthal quantum number had to be determined by a transcendental equation, which was implemented in the calculation through use of the so-called argument principle [39], which is just the residue theorem.

In this paper, we further illustrate this nontrivial azimuthal dependence by considering a similar wedge geometry, in which the infinite wedge is formed by two planar δ-function potentials, making a dihedral angle $\alpha \in [0, \pi]$, closed by a coaxial Dirichlet circular cylinder of radius a. See Fig. 1. We calculate the Casimir energy of a massless scalar field subject to these boundary conditions. Because that energy is divergent, we compute the energy relative to that when the radius of the cylinder is infinite, and when neither or only one of the wedge boundaries is present. Thus, we are computing the energy of mutual interaction between the three boundaries. The results, which are rather easily found numerically, are very similar to those found for the electromagnetic field in a perfectly conducting cylinder with a magnetodielectric wedge, as considered in Ref. [38]. We describe the geometry in terms of cylindrical coordinates (ρ, θ, z) with the origin lying along the cylinder axis.

Because the interest in this problem largely lies in the angular dependence, it is natural to approach the problem in an unconventional way, in which the reduced Green's function refers to the azimuthal, not the radial, coordinate. Technically, that approach requires consideration of an annular region, which we describe in Sec. IV. This approach also allows use of the multiple-scattering technique, and should have application to more complicated geometries, such as the interaction between hyperboloids. We can think of the radial planes between the concentric cylinders
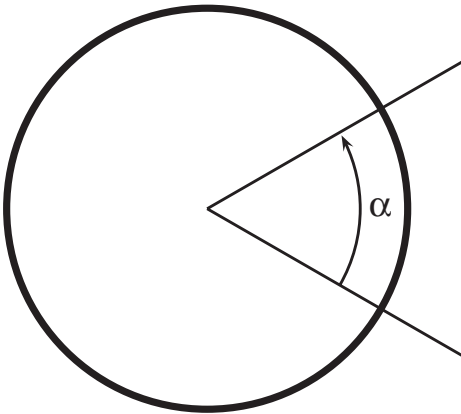

FIG. 1. A Dirichlet cylinder intersecting with a coaxial wedge made of semitransparent plates.

as forming an annular piston, and we have computed numerically the Casimir attractive torque between those planes. An alternative approach to the determination of the Casimir energy for any such angular potential is described in Sec. V. The radial functions encountered in these wedge problems are modified Bessel functions of imaginary order; since these are rather infrequently described in the literature, we collect some relevant properties in Appendix B. Required integrals over the squared radial functions may be evaluated using identities described in Appendix A.

II. SEMITRANSPARENT WEDGE

In this paper we consider a massless scalar model, in which the wedge is described by a δ-function potential, $V(\rho, \theta) = v(\theta)/\rho^2$,

$$v(\theta) = \lambda_1 \delta(\theta - \alpha/2) + \lambda_2 \delta(\theta + \alpha/2). \quad (2.1)$$

This has the diaphanous property of preserving the speed of light both within and outside the wedge. This wedge is superimposed on a coaxial circular cylindrical shell, of radius a, on which the scalar field ϕ vanishes. To calculate the Casimir energy, we can use the formula [2]

$$E = \frac{1}{2i} \int_{-\infty}^{\infty} \frac{d\omega}{2\pi} \int (d\mathbf{r}) 2\omega^2 \mathcal{G}(\mathbf{r}, \mathbf{r}; \omega), \quad (2.2)$$

where $\mathcal{G}$ is the Green's function for the situation under consideration, satisfying

$$(-\nabla^2 + V(\rho, \theta) - \omega^2)\mathcal{G}(\mathbf{r}, \mathbf{r}'; \omega) = \delta(\mathbf{r} - \mathbf{r}'). \quad (2.3)$$

We can solve this cylindrical problem in terms of the two-dimensional Green's function G,

$$\mathcal{G}(\mathbf{r}, \mathbf{r}'; \omega) = \int_{-\infty}^{\infty} \frac{dk_z}{2\pi} e^{ik_z(z-z')} G(\rho, \theta; \rho', \theta'), \quad (2.4)$$

which satisfies

$$\left[-\frac{1}{\rho} \frac{\partial}{\partial \rho} \rho \frac{\partial}{\partial \rho} + \kappa^2 - \frac{1}{\rho^2} \frac{\partial^2}{\partial \theta^2} + \frac{v(\theta)}{\rho^2} \right] G(\rho, \theta; \rho', \theta')$$
$$= \frac{1}{\rho} \delta(\rho - \rho')\delta(\theta - \theta'), \quad (2.5)$$

where $\kappa^2 = k_z^2 - \omega^2$. This separates into two equations, one for the angular eigenfunction $\Theta_\nu(\theta)$,

$$\left[-\frac{\partial^2}{\partial \theta^2} + v(\theta) \right] \Theta_\nu(\theta) = \nu^2 \Theta_\nu(\theta), \quad (2.6)$$

where we have assumed that the azimuthal eigenfunctions are normalized according to

$$\int_{-\pi}^{\pi} d\theta \Theta_\nu(\theta)\Theta_{\nu'}^*(\theta) = \delta_{\nu\nu'}; \quad (2.7)$$

orthogonality of the eigenfunctions follows from the Sturm-Liouville nature of the problem. Now the two-dimensional Green's function can be constructed as

$$G(\rho, \theta; \rho', \theta') = \sum_\nu \Theta_\nu(\theta)\Theta_\nu^*(\theta')g_\nu(\rho, \rho'). \qquad (2.8)$$

The radial reduced Green's function satisfies

$$\left[-\frac{1}{\rho}\frac{\partial}{\partial\rho}\rho\frac{\partial}{\partial\rho} + \kappa^2 + \frac{\nu^2}{\rho^2}\right]g_\nu(\rho, \rho') = \frac{1}{\rho}\delta(\rho - \rho').$$

$$(2.9)$$

The latter, for a Dirichlet circle at $\rho = a$, has the familiar solution,

$$g_\nu(\rho, \rho') = I_\nu(\kappa\rho_<)K_\nu(\kappa\rho_>) - I_\nu(\kappa\rho)I_\nu(\kappa\rho')\frac{K_\nu(\kappa a)}{I_\nu(\kappa a)},$$

$$\rho, \rho' < a, \qquad (2.10a)$$

$$g_\nu(\rho, \rho') = I_\nu(\kappa\rho_<)K_\nu(\kappa\rho_>) - K_\nu(\kappa\rho)K_\nu(\kappa\rho')\frac{I_\nu(\kappa a)}{K_\nu(\kappa a)},$$

$$\rho, \rho' > a. \qquad (2.10b)$$

The azimuthal eigenvalue ν is determined by Eq. (2.6). For the wedge δ-function potential (2.1) it is easy to determine ν by writing the solutions to Eq. (2.6) as linear combinations of $e^{\pm i\nu\theta}$, with different coefficients in the sectors $|\theta| < \alpha/2$ and $\pi \geq |\theta| > \alpha/2$. Continuity of the function, and discontinuity of its derivative, are imposed at the wedge boundaries. The four simultaneous linear homogeneous equations have a solution only if the secular equation is satisfied:

$$0 = D(\nu)$$

$$= \sin^2\nu(\alpha - \pi) - \left(1 - \frac{4\nu^2}{\lambda_1\lambda_2}\right)\sin^2\pi\nu$$

$$- \left(\frac{\nu}{\lambda_1} + \frac{\nu}{\lambda_2}\right)\sin 2\pi\nu. \qquad (2.11)$$

Because we recognize that the reflection coefficient for a single δ-function interface is $r_i = (1 + 2i\nu/\lambda_i)^{-1}$, implying that

$$\text{Re}\,(r_1^{-1}r_2^{-1}) = 1 - \frac{4\nu^2}{\lambda_1\lambda_2}, \qquad \text{Im}(r_1^{-1}r_2^{-1}) = \frac{2\nu}{\lambda_1} + \frac{2\nu}{\lambda_2},$$

$$(2.12)$$

we see that this dispersion relation coincides with that found in Ref. [38] when the reflection coefficient is purely real. Note that the $\nu = 0$ root of Eq. (2.11) is spurious and must be excluded; unlike for the magnetodielectric wedge, there are no $\nu = 0$ modes for the semitransparent wedge.

Now using the general formula (2.2) we compute the Casimir energy per length from

$$\mathcal{E} = \frac{1}{2i}\int_{-\infty}^{\infty}\frac{d\omega}{2\pi}2\omega^2\int_{-\infty}^{\infty}\frac{dk}{2\pi}\sum_\nu\int_0^\infty d\rho\rho g_\nu(\rho, \rho).$$

$$(2.13)$$

Note that we do not need to know the eigenfunctions Θ_ν, only the eigenvalues ν.

The apparent difficulty, that the eigenvalue condition for ν cannot be explicitly solved, may be resolved through enforcing the eigenvalue condition by the argument principle [39–44], which gives a sum over nonexplicit eigenvalues in terms of a contour integral around the real line,

$$\sum_\nu f(\nu) = \frac{1}{2\pi i}\int_\gamma d\nu\left(\frac{d}{d\nu}\ln D(\nu)\right)f(\nu). \qquad (2.14)$$

The contour of integration γ is illustrated in Fig. 2. Thus, we have the expression after making the Euclidean rotation, $\omega \to i\zeta$, and converting to polar coordinates,

$$\zeta = \kappa\cos\varphi, \qquad k = \kappa\sin\varphi, \qquad (2.15)$$

$$\mathcal{E} = -\frac{1}{8\pi^2 i}\int_0^\infty d\kappa\kappa^3\int_\gamma d\nu\left(\frac{d}{d\nu}\ln D(\nu)\right)$$

$$\times \int_0^\infty d\rho\rho g_\nu(\rho, \rho). \qquad (2.16)$$

This formal expression is rather evidently divergent. We are seeking the mutual interaction energy due to the three boundaries, the two sides of the wedge and the circular arc. Therefore, we first must subtract off the free radial Green's function without the circle at $\rho = a$, which then implies

$$\int_0^\infty d\rho\rho g_\nu(\rho, \rho) \to \frac{a}{2\kappa}\frac{d}{d\kappa a}\ln[I_\nu(\kappa a)K_\nu(\kappa a)]. \quad (2.17)$$

(The familiar form of this expression is quite general, as illustrated in Appendix A.) We further want to remove the term present without the wedge potential:
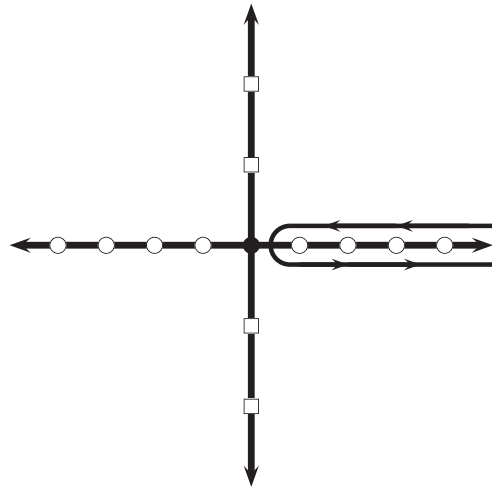

FIG. 2. Contour of integration γ for the argument principle (2.14). Shown also are singularities of the integrand (2.16) along the real and imaginary ν axes.

$$D(\nu) \to \tilde{D}(\nu) = \frac{\lambda_1 \lambda_2}{4\nu^2} \frac{D(\nu)}{\sin^2 \pi \nu}. \qquad (2.18)$$

The resulting energy is still not finite. The reason is that it contains the self-energy of a single δ-function potential crossed by the circular cylinder.

Therefore, we still must remove that part of $\tilde{D}$ due to a single potential, which may be obtained by setting λ_2 (or

λ_1) equal to zero:

$$\tilde{D}_1(\nu) = 1 - \frac{\lambda_1}{2\nu} \cot\nu\pi, \qquad (2.19)$$

so the final form of the dispersion function is obtained by replacing

$$\tilde{D}(\nu) \to \hat{D}(\nu) = \frac{\tilde{D}(\nu)}{\tilde{D}_1(\nu)\tilde{D}_2(\nu)} = \frac{\lambda_1 \lambda_2 \sin^2 \nu(\alpha - \pi)/\sin^2 \nu\pi + 4\nu^2 - \lambda_1\lambda_2 - 2\nu(\lambda_1 + \lambda_2)\cot\nu\pi}{(2\nu - \lambda_1 \cot\nu\pi)(2\nu - \lambda_2 \cot\nu\pi)}. \qquad (2.20)$$

(Although the spurious $\nu = 0$ root is still present, it may be checked that this gives rise to an irrelevant divergent constant in the energy.)

It is now easy to see that the integrand in the expression for the energy falls off exponentially fast for large ν in the right-half complex ν plane, except along the real ν axis, where an exponential convergence factor may be inserted. In particular, for $\nu = i\eta$, $\eta \gg 1$, $\hat{D}(i\eta)$ differs only exponentially from unity:

$$\hat{D}(i\eta) \sim 1 - \frac{\lambda_1 \lambda_2}{(2\eta + \lambda_1)(2\eta + \lambda_2)} e^{-2\eta\alpha}. \qquad (2.21)$$

Then it is permissible to unfold γ and convert the contour to one running parallel to the imaginary axis as shown in Fig. 3. For imaginary ν, $\nu = i\eta$, the dispersion functions become

$$\tilde{D}_1(i\eta) = 1 + \frac{\lambda_1}{2\eta} \coth\eta\pi, \qquad (2.22)$$

and

$$\hat{D}(i\eta) = \frac{-\lambda_1 \lambda_2 \sinh^2 \eta(\alpha - \pi)/\sinh^2 \eta\pi + 4\eta^2 + \lambda_1\lambda_2 + 2\eta(\lambda_1 + \lambda_2)\coth\eta\pi}{(2\eta + \lambda_1 \coth\eta\pi)(2\eta + \lambda_2 \coth\eta\pi)}. \qquad (2.23)$$

Because of Eq. (2.21), the resulting expression for the Casimir energy is manifestly convergent. This can be further simplified by noting that $\frac{d}{d\eta} \ln\hat{D}(i\eta)$ is odd, which eliminates the K_ν in Eq. (2.17), and then yields the expression

$$\mathcal{E} = \frac{1}{8\pi^2 a^2} \int_0^\infty dx x^2 \int_0^\infty d\eta \left(\frac{d}{d\eta} \ln\hat{D}(i\eta)\right)$$
$$\times \frac{d}{dx} \arctan\frac{K_{i\eta}(x)}{L_{i\eta}(x)}, \qquad (2.24)$$

in terms of

$$K_\mu(x) = -\frac{\pi}{2\sin\pi\mu}[I_\mu(x) - I_{-\mu}(x)], \qquad (2.25a)$$

$$L_\mu(x) = \frac{i\pi}{2\sin\pi\mu}[I_\mu(x) + I_{-\mu}(x)], \qquad (2.25b)$$

where both $L_{i\eta}(x)$ and $K_{i\eta}(x)$ are real for real η and x, and

$$I_{i\eta}(x) = \frac{\sinh\eta\pi}{\pi}[L_{i\eta}(x) - iK_{i\eta}(x)]. \qquad (2.26)$$

We should further note that the arctangent appearing in Eq. (2.24) is not the principal value, but rather the smooth function in which the phase is accumulated. (Some prop-

erties of the modified Bessel functions of imaginary order are collected in Appendix B.)

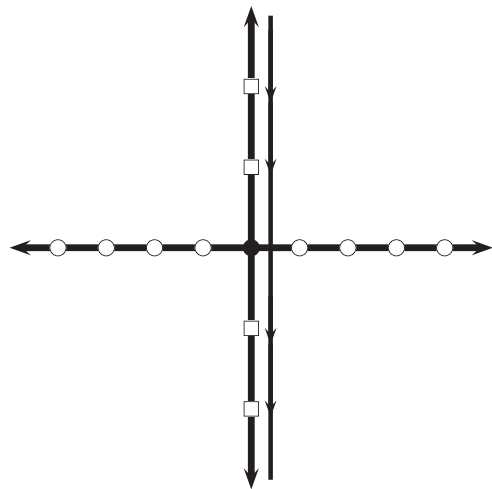Now we turn to the numerical evaluation of this expression.

FIG. 3. Contour of integration for the η integral in Eq. (2.24).

III. NUMERICAL EVALUATION OF CASIMIR ENERGY FOR THE SEMITRANSPARENT WEDGE

It is actually quite easy to evaluate Eq. (2.24), because the $\frac{d}{d\eta}\log\hat{D}$ function is strongly peaked for small η, except for extremely small values of the dihedral angle α. The difficulty numerically is that $K_{i\eta}(x)/L_{i\eta}(x)$ is an extremely oscillatory function of x for $x < \eta$, becoming infinitely oscillatory as $x \rightarrow 0$. For $x > \eta$, the ratio of modified Bessel functions of imaginary order monotonically and exponentially approaches zero. (For incomplete asymptotic information about Bessel functions of imaginary order see Refs. [45,46]; see also Appendix B.) The function

$$h(\eta) = \int_0^\infty dx x^2 \frac{d}{dx} \arctan\frac{K_{i\eta}(x)}{L_{i\eta}(x)}, \qquad (3.1)$$

however, is very smooth. (It vanishes at $\eta = 0$, so the spurious zero mode should not contribute.) To evaluate the double integral, we compute h at a finite number of discrete points, form a spline approximation which is indistinguishable from h, and then evaluate the function

$$e(\alpha) = \int_0^\infty d\eta h(\eta) \frac{d}{d\eta} \ln\hat{D}(i\eta), \qquad (3.2)$$

numerically. (This strategy is similar to that employed in Ref. [38].) The integrand here is quite strongly peaked in a neighborhood of the origin. The Casimir energy, with the indicated subtractions, is

$$\mathcal{E} = \frac{1}{8\pi^2 a^2} e(\alpha). \qquad (3.3)$$

The results found by this strategy are shown in Figs. 4 and 5.

These graphs are very reminiscent of those found in Ref. [38] for the magnetodielectric wedge. In particular, we note that the energies are finite for all α, but as $\lambda \rightarrow \infty$, the limit corresponding to a Dirichlet boundary, the energy
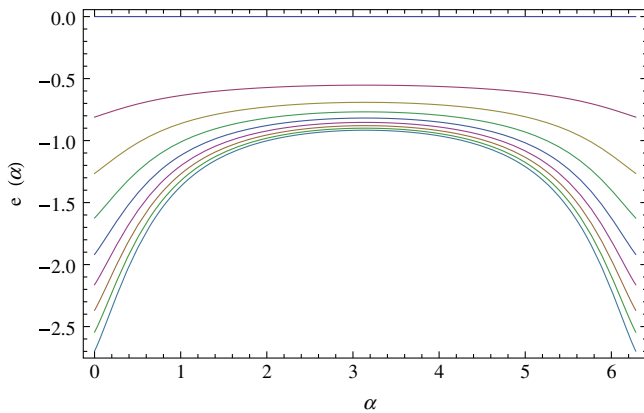

FIG. 4 (color online). Casimir energy for a semitransparent wedge embedded in a Dirichlet cylinder, as a function of the dihedral angle α. Shown in order from highest to lowest are the energies (3.3) for $\lambda_1 = \lambda_2 = 0.5$ to 4.0, by steps of 0.5.
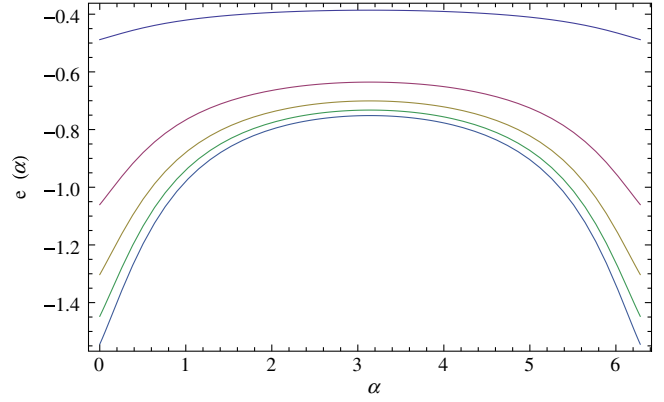

FIG. 5 (color online). Casimir energy for a semitransparent wedge embedded in a Dirichlet cylinder, as a function of the dihedral angle α. Shown in order from highest to lowest are the energies (3.3) for $\lambda_1 = 1$ and $\lambda_2 = 0.1$ to 2.1, by steps of 0.5.

diverges as $\alpha \rightarrow 0$ or 2π; the same phenomena was observed in Ref. [38] for the perfectly conducting wedge limit, treated previously in Ref. [37]. This energy should be observable as a torque on the two semitransparent plates, $\tau(\alpha) = -\frac{\partial}{\partial\alpha}\mathcal{E}(\alpha)$, which is, as expected, attractive. (The divergence associated with the apex of the wedge has been subtracted.)

IV. ALTERNATIVE CALCULATION OF CASIMIR ENERGY FOR SEMITRANSPARENT WEDGE IN AN ANNULUS

We start from the formula (2.2) for the Casimir energy in terms of the Green's function,

$$E = \frac{1}{2i} \int \frac{d\omega}{2\pi} 2\omega^2 \text{Tr}(\mathcal{G} - \mathcal{G}^{(0)}), \qquad (4.1)$$

where the trace denotes the integration over spatial coordinates, and we have again subtracted out the vacuum contribution. The Green's function $\mathcal{G}(\mathbf{r}, \mathbf{r}')$ will satisfy the equation

$$[-\nabla^2 - \omega^2 + V(\mathbf{r})]\mathcal{G}(\mathbf{r}, \mathbf{r}') = \delta(\mathbf{r} - \mathbf{r}'), \qquad (4.2)$$

while the free Green's function $\mathcal{G}^{(0)}$ satisfies the same equation with $V(\mathbf{r}) = 0$. Once again we specialize to the cylindrical geometry, but now defined in an annulus. Specifically, we require that the boundary conditions on the Green's function are that it vanishes at $\rho = a$ and $\rho = b$ with $b > a$; that is, it satisfies Dirichlet boundary conditions on two concentric circles. (We will see the necessity for both an inner and an outer boundary in the following.) If the potential has the form $V(\mathbf{r}) = v(\theta)/\rho^2$, then we can use separation of variables to write the Green's function as, in terms of the separation constant η,
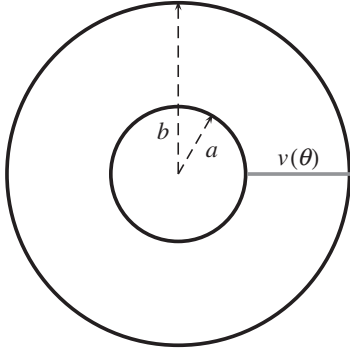
FIG. 6.   The annular geometry considered.

$$\mathcal{G}(\mathbf{r}, \mathbf{r}'; \omega) = \int_{-\infty}^{\infty} \frac{dk_z}{2\pi} e^{ik_z(z-z')} \sum_{\eta} R_\eta(\rho; \omega, k_z)$$
$$\times R_\eta(\rho'; \omega, k_z) g_\eta(\theta, \theta'). \qquad (4.3)$$

The geometry we are considering is illustrated in Fig. 6. Note that instead of expanding in eigenfunctions of θ as in Eq. (2.8), we have expanded in terms of radial eigenfunctions. (This cannot be done without the inner boundary—that is, this alternative separation works for an annulus but not for a disk.) The R functions are normalized radial eigenfunctions of the eigenvalue problem,

$$\left[-\rho \frac{d}{d\rho} \rho \frac{d}{d\rho} - (\omega^2 - k_z^2)\rho^2 \right] R_\eta(\rho; \omega, k_z)$$
$$= \eta^2 R_\eta(\rho; \omega, k_z), \qquad (4.4)$$

with boundary values $R_\eta(a; \omega, k_z) = R_\eta(b; \omega, k_z) = 0$. The g_η is the reduced Green's function in the azimuthal coordinates that satisfies the equation

$$\left[-\frac{d^2}{d\theta^2} + \eta^2 + v(\theta) \right] g_\eta(\theta, \theta') = \delta(\theta - \theta'), \qquad (4.5)$$

with periodic boundary conditions. Finally inserting Eq. (4.3) into Eq. (4.1) we get an expression for the vacuum energy

$$E = \frac{1}{2i} \int_{-\infty}^{\infty} \frac{d\omega}{2\pi} 2\omega^2 \int_{-\infty}^{\infty} \frac{dk_z}{2\pi} \int dz \sum_{\eta} \int_a^b \rho d\rho$$
$$\times R_\eta^2(\rho; \omega, k_z) \int d\theta [g_\eta(\theta, \theta) - g_\eta^{(0)}(\theta, \theta)]. \qquad (4.6)$$

We can simplify the result considerably if we now make a Euclidean rotation from $\omega \to i\zeta$, make the substitution $\zeta^2 + k_z^2 = \kappa^2$, and integrate out the angle in the ζ-k_z plane to get the expression for the energy per unit length

$$\mathcal{E} = -\frac{1}{4\pi} \int_0^{\infty} \kappa^3 d\kappa \sum_{\eta} \int_a^b \rho d\rho R_\eta^2(\rho; \kappa)$$
$$\times \int d\theta [g_\eta(\theta, \theta) - g_\eta^{(0)}(\theta, \theta)]. \qquad (4.7)$$

A. The radial eigenvalue problem

We see that we need an expression for the radial integral

$$\int_a^b \rho d\rho R_\eta^2(\rho; \kappa), \qquad (4.8)$$

where the R_η's are the normalized eigenfunctions obeying the differential equation (4.4). The normalization is

$$\int_a^b \frac{d\rho}{\rho} R_\eta^2(\rho; \kappa) = 1. \qquad (4.9)$$

To evaluate this integral we will use the identity (A9). The boundary conditions are that $R_\eta(a; \kappa) = R_\eta(b; \kappa) = 0$; this is only possible for discrete values of η—namely, this is an eigenvalue condition for η. Let $\tilde{R}_\eta(r; \kappa)$ be a solution to Eq. (4.4) which satisfies $\tilde{R}_\eta(a; \kappa) = 0$ for all η and κ. The normalized solution can then be written as

$$R_\eta(\rho; \kappa) = \frac{1}{N} \tilde{R}_\eta(\rho; \kappa), \qquad (4.10)$$

where

$$N^2 = \int_a^b \frac{d\rho}{\rho} \tilde{R}_\eta^2(\rho, \kappa). \qquad (4.11)$$

Now writing Eq. (4.4) as

$$\left[-\frac{d}{d\rho} \rho \frac{d}{d\rho} + \kappa^2 \rho - \eta^2 \left(\frac{1}{\rho} \right) \right] R_\eta(\rho, \kappa) = 0, \qquad (4.12)$$

we can see that $\frac{1}{\rho} \tilde{R}_\eta^2(\rho; \kappa)$ is a total derivative given by Eq. (A9). (We replace $\kappa \to \eta$ there.) The integral (4.11) is now trivial to carry out. We see that the value at the lower limit of integration is zero by our boundary condition that $\tilde{R}_\eta(a; \kappa) = 0$, and the second term on the right in Eq. (A9) at the upper limit is zero by the eigenvalue condition $\tilde{R}_\eta(b; \kappa) = 0$. This gives the normalization constant as

$$N^2 = \frac{b}{2\eta} \frac{\partial}{\partial b} \tilde{R}_\eta(b; \kappa) \frac{\partial}{\partial \eta} \tilde{R}_\eta(b; \kappa). \qquad (4.13)$$

Now by considering κ rather than η as the parameter in Eq. (4.12), we also have from Eq. (A9) that the desired integrand in (4.8) is a total derivative,

$$\int_a^b \rho d\rho \tilde{R}_\eta^2(\rho, \kappa) = -\frac{b}{2\kappa} \frac{\partial}{\partial b} \tilde{R}_\eta(b; \kappa) \frac{\partial}{\partial \kappa} \tilde{R}_\eta(b; \kappa). \qquad (4.14)$$

So the desired integral given by Eq. (4.8) can be concisely written as

$$\int_a^b \rho d\rho R_\eta^2(\rho; \kappa) = -\frac{\eta}{\kappa} \frac{\frac{\partial}{\partial \kappa} \tilde{R}_\eta(b; \kappa)}{\frac{\partial}{\partial \eta} \tilde{R}_\eta(b; \kappa)}. \qquad (4.15)$$

B. Argument principle

Now we again use the argument principle (2.14), which we previously used for the angular eigenvalues; in this case

the sum is over the radial eigenvalues, and the eigenvalue condition is given by $D(\eta) = R_\eta(b; \kappa)$. So we have occurring in the energy (4.7) the form

$$\sum_\eta \int_a^b \rho d\rho R_\eta^2(\rho; \kappa)$$

$$= \frac{1}{2\pi i} \int_\gamma d\eta \frac{\frac{\partial}{\partial \eta}\tilde{R}_\eta(b; \kappa)}{\tilde{R}_\eta(b; \kappa)}\left(-\frac{\eta}{\kappa}\frac{\frac{\partial}{\partial \kappa}\tilde{R}_\eta(b; \kappa)}{\frac{\partial}{\partial \eta}\tilde{R}_\eta(b; \kappa)}\right)$$

$$= -\frac{1}{2\pi i}\int_\gamma d\eta \frac{\eta}{\kappa}\frac{\partial}{\partial \kappa}\ln\tilde{R}_\eta(b; \kappa). \quad (4.16)$$

The expression for the Casimir energy per length (4.7) is then given by

$$\mathcal{E} = \frac{1}{8\pi^2 i}\int_0^\infty \kappa^2 d\kappa \int_\gamma \eta d\eta\left(\frac{\partial}{\partial \kappa}\ln\tilde{R}_\eta(b; \kappa)\right)$$

$$\times \int d\theta(g_\eta(\theta, \theta) - g_\eta^{(0)}(\theta, \theta)). \quad (4.17)$$

C. The radial solutions

The differential equation (4.12) is the modified Bessel differential equation, of imaginary order. We need two independent solutions of this equation, which we could take to be $K_{i\eta}(\kappa\rho)$ and $L_{i\eta}(\kappa\rho)$, given by Eq. (2.25). Now

we want to find the solution $\tilde{R}_\eta(\rho; \kappa)$ that is zero for $\rho = a$ for all values of η and κ. An obvious solution is

$$\tilde{R}_\eta(\rho; \kappa) = K_{i\eta}(\kappa a)\tilde{I}_{i\eta}(\kappa\rho) - \tilde{I}_{i\eta}(\kappa a)K_{i\eta}(\kappa\rho)$$

$$= R_{-\eta}(\rho, \kappa), \quad (4.18)$$

where

$$\tilde{I}_\nu = \frac{1}{2}(I_\nu + I_{-\nu}) = \frac{\sin\nu\pi}{i\pi}L_\nu \quad (4.19)$$

is the function initially called L_ν in Ref. [38]; here this is a more convenient choice, in that both K_ν and $\tilde{I}_\nu$ are even in ν.

D. Reduced Green's function

We also need the reduced Green's function in the angular coordinates. The free Green's function is easily found to be

$$g_\eta^{(0)}(\theta, \theta') = \frac{1}{2\eta}\left(-\sinh\eta|\theta - \theta'|\right.$$

$$\left. + \frac{\cosh\eta\pi}{\sinh\eta\pi}\cosh\eta|\theta - \theta'|\right). \quad (4.20)$$

If we assume a single δ-function potential $v(\theta) = \lambda\delta(\theta - \alpha)$, then the Green's function is

$$g_\eta(\theta, \theta') = \frac{1}{2\eta}\left(-\sinh\eta|\theta - \theta'| + \frac{1}{2\eta\sinh\eta\pi + \lambda\cosh\eta\pi}\right.$$

$$\left.\times\left[2\eta\cosh\eta\pi\cosh\eta|\theta - \theta'| - \frac{\lambda}{2\sinh\eta\pi}\{\cosh\eta(2\pi + 2\alpha - \theta - \theta') - \cosh2\eta\pi\cosh\eta|\theta - \theta'|\}\right]\right), \quad (4.21)$$

which is defined for θ and θ' in the interval $[\alpha, 2\pi + \alpha]$.

The quantity of interest, $\text{tr}(g - g^{(0)})$, is then

$$\int_\alpha^{2\pi+\alpha} d\theta[g_\eta(\theta, \theta) - g_\eta^{(0)}(\theta, \theta)]$$

$$= \frac{-\lambda(\sinh\eta\pi\cosh\eta\pi + \eta\pi)}{2\eta^2\sinh\eta\pi(2\eta\sinh\eta\pi + \lambda\cosh\eta\pi)}, \quad (4.22)$$

and this expression can be seen to be a total derivative

$$\int_\alpha^{2\pi+\alpha} d\theta[g_\eta(\theta, \theta) - g_\eta^{(0)}(\theta, \theta)]$$

$$= \frac{1}{2\eta}\frac{\partial}{\partial\eta}\ln\left(1 + \frac{\lambda}{2\eta}\coth\eta\pi\right)$$

$$= \frac{1}{2\eta}\frac{\partial}{\partial\eta}\ln(1 + \lambda g_\eta^{(0)}(\alpha, \alpha)), \quad (4.23)$$

which agrees with the result stated in Eq. (2.22). It is precisely of the expected form (A11).

E. Casimir energy

The final form for the Casimir energy for a single radial δ-function potential in the annular region is

$$\mathcal{E} = \frac{1}{16\pi^2 i}\int_0^\infty \kappa^2 d\kappa \int_\gamma d\eta\left(\frac{\partial}{\partial\kappa}\ln[K_{i\eta}(\kappa a)\tilde{I}_{i\eta}(\kappa b)\right.$$

$$\left. - \tilde{I}_{i\eta}(\kappa a)K_{i\eta}(\kappa b)]\right)\left(\frac{\partial}{\partial\eta}\ln\left[1 + \frac{\lambda}{2\eta}\coth\eta\pi\right]\right). \quad (4.24)$$

This result may also be obtained by the multiple-scattering formalism [47], which says that

$$E = -\frac{1}{2i}\text{Tr}\ln GG^{(0)-1} = \frac{1}{2i}\text{Tr}\ln(1 + G^{(0)}V), \quad (4.25)$$

the latter form being a useful form for a single potential. We see that Eq. (4.24) exactly corresponds to this if we integrate by parts on η and κ:
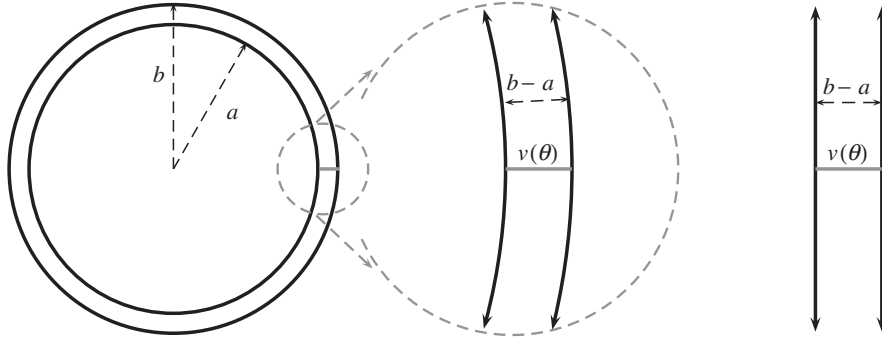
FIG. 7.   Large radius limit of annular geometry. For large annular radii a and b, with $b - a$ fixed, the annular boundaries become indistinguishable from parallel planes.

$$\mathcal{E} = \frac{1}{8\pi^2 i} \int_0^\infty d\kappa \kappa \int_\gamma d\eta \left(\frac{\partial}{\partial\eta} \ln[K_{i\eta}(\kappa a)\tilde{I}_{i\eta}(\kappa b)\right.$$
$$\left. - \tilde{I}_{i\eta}(\kappa a)K_{i\eta}(\kappa b)]\right) \ln[1 + \lambda g^{(0)}(\alpha, \alpha)]. \quad (4.26)$$

We can check this result by taking the limit as a and b get very large, but with fixed distance between the circles. In this limit this result should reproduce the case of a single semitransparent plane between two parallel Dirichlet planes, as illustrated in Fig. 7. The energy in that case should be

$$\mathcal{E} = -\frac{1}{8\pi} \int_0^\infty \kappa^3 d\kappa \sum_{n=1}^\infty \frac{1}{\tilde{\eta}} \frac{\partial}{\partial\tilde{\eta}} \ln\left(1 + \frac{\tilde{\lambda}}{2\tilde{\eta}}\right), \quad (4.27)$$

where $\tilde{\eta}^2 = \kappa^2 + (n\pi/(b-a))^2$. If we use the argument principle we can write it as

$$\mathcal{E} = -\frac{1}{16\pi^2 i} \int_0^\infty \kappa^3 d\kappa \int_\gamma d\tilde{\eta}$$
$$\times \left(\frac{\partial}{\partial\tilde{\eta}} \ln\left[\frac{\sin\sqrt{\tilde{\eta}^2 - \kappa^2}(b-a)}{\sqrt{\tilde{\eta}^2 - \kappa^2}}\right]\right)$$
$$\times \left(\frac{1}{\tilde{\eta}} \frac{\partial}{\partial\tilde{\eta}} \ln\left[1 + \frac{\tilde{\lambda}}{2\tilde{\eta}}\right]\right). \quad (4.28)$$

The square root divided out in the logarithm is present to remove the spurious square-root singularity. It should be noted that both of these expressions (4.24) and (4.28) are divergent, but the divergence is simply the self-energy divergence always present with a single plane.

It is straightforward to prove that Eq. (4.24) reduces to Eq. (4.28) in the appropriate limit. The second logarithm in the former becomes, in the limit $\eta \to \infty$, simply $\ln(1 + \lambda/2\eta)$, so that suggests the correspondence

$$\tilde{\eta} = \frac{\eta}{a}, \qquad \tilde{\lambda} = \frac{\lambda}{a}. \quad (4.29)$$

And the leading uniform asymptotic expansion of the modified Bessel functions [45,46] gives

$$K_{i\eta}\left(\eta\frac{\kappa a}{\eta}\right)\tilde{I}_{i\eta}\left(\eta\frac{\kappa b}{\eta}\right) - K_{i\eta}\left(\eta\frac{\kappa b}{\eta}\right)\tilde{I}_{i\eta}\left(\eta\frac{\kappa a}{\eta}\right)$$
$$\sim \frac{1}{2\eta} t(z_a)^{1/2} t(z_b)^{1/2} \sin[\eta(f(z_a) - f(z_b))], \quad (4.30)$$

where $z_a = \kappa a/\eta$, $z_b = \kappa b/\eta$, $t(z) = (1 - z^2)^{-1/2}$, and

$$f(z) = \ln\left(\frac{1 + t(z)^{-1}}{z}\right) - \frac{1}{t(z)}, \qquad f'(z) = -\frac{1}{zt(z)}. \quad (4.31)$$

(The function f is a continuation of a function usually called η, but we have already used that symbol repeatedly.) This result holds true for $z < 1$, but an equivalent form, obtained by analytic continuation, holds for $z > 1$. (See Appendix B.) Then the derivative with respect to κ term in Eq. (4.24) becomes

$$\frac{\partial}{\partial\kappa} \ln(K\tilde{I} - \tilde{I}K) \sim \frac{\partial}{\partial\kappa} \ln\left[\frac{1}{\sqrt{\eta^2 - (\kappa a)^2}}\right.$$
$$\left. \times \sin\left(\sqrt{\eta^2 - (\kappa a)^2}\frac{b-a}{b}\right)\right], \quad (4.32)$$

so with the substitutions (4.29), and the observation that

$$\frac{\partial}{\partial\eta} F(\eta^2 - \kappa^2) = -\frac{\eta}{\kappa} \frac{\partial}{\partial\kappa} F(\eta^2 - \kappa^2), \quad (4.33)$$

we exactly recover the Casimir energy for a semitransparent plate between two Dirichlet plates (4.28).

It is also easy to check that the energy (4.24) agrees with the expression for the energy given by the more conventional approach described in Sec. II. The latter is

$$\mathcal{E} = -\frac{1}{16\pi^2 i} \int_0^\infty \kappa^2 d\kappa \int_\gamma d\nu \left(\frac{\partial}{\partial\nu} \ln\left[1 - \frac{\lambda}{2\nu} \cot\nu\pi\right]\right)$$
$$\times \frac{\partial}{\partial\kappa} \ln[I_\nu(\kappa a)K_\nu(\kappa b) - I_\nu(\kappa b)K_\nu(\kappa a)]. \quad (4.34)$$

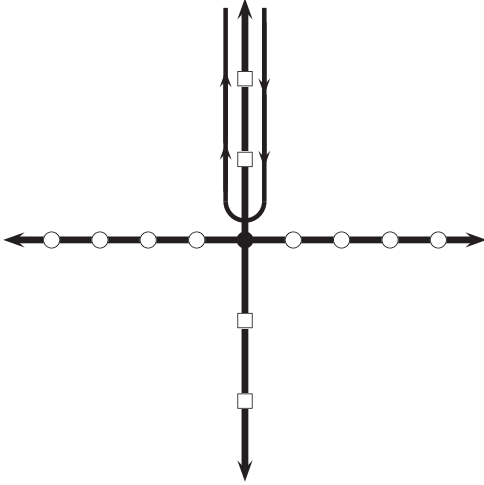This equivalence may be easily shown by seeing that the integrand is odd in ν, because

FIG. 8.   Transformed contour of integration for the ν integral in Eq. (4.34).

$$I_\nu(\kappa a)K_\nu(\kappa b) - I_\nu(\kappa b)K_\nu(\kappa a)$$
$$= \tilde{I}_\nu(\kappa a)K_\nu(\kappa b) - \tilde{I}_\nu(\kappa b)K_\nu(\kappa a), \qquad (4.35)$$

and then rotating the contour γ from that shown in Fig. 2 to that in Fig. 3, which may then be transformed to that shown in Fig. 8, by changing ν to $-\nu$ on the negative imaginary axis. Thus the contour γ in the ν plane is transformed to γ in the η plane appearing in Eq. (4.24) (except traversed in the opposite sense), and the equivalence is established.

F. Interaction between two semitransparent planes

If we want to look at an explicitly finite quantity we will need to look at the interaction energy between two semi-
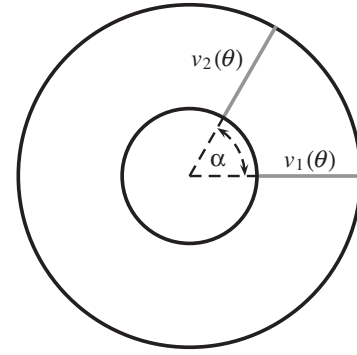

FIG. 9.   Two semitransparent plates in an annulus.

transparent planes. The geometry is illustrated in Fig. 9. We will use a slightly different form of the energy for this, based on the multiple-scattering formalism [47]:

$$E = \frac{1}{2i} \int_{-\infty}^{\infty} \frac{d\omega}{2\pi} \, \mathrm{Tr} \ln(1 - \mathcal{G}^{(1)}V_1\mathcal{G}^{(2)}V_2). \qquad (4.36)$$

The subscripts on the V's represent the potentials $V_1(\mathbf{r}) = \lambda_1\delta(\theta)/\rho^2$, and $V_2(\mathbf{r}) = \lambda_2\delta(\theta - \alpha)/\rho^2$. The Green's functions with superscript (i) represent the interaction with only a single potential V_i. By using Eq. (4.3), we can greatly simplify the interaction energy to

$$\mathcal{E} = \frac{1}{4\pi} \int_0^\infty \kappa d\kappa \sum_\eta \ln(1 - \mathrm{tr}g_\eta^{(1)} v_1 g_\eta^{(2)} v_2). \qquad (4.37)$$

We already have an expression for $g_\eta^{(i)}$, given in Eq. (4.21). Using the latter we can write

$$\mathrm{tr}\, g_\eta^{(1)} v_1 g_\eta^{(2)} v_2 = \frac{\lambda_1\lambda_2\cosh^2\eta(\pi - \alpha)}{(2\eta\sinh\eta\pi + \lambda_1\cosh\eta\pi)(2\eta\sinh\eta\pi + \lambda_2\cosh\eta\pi)}. \qquad (4.38)$$

This exactly agrees with Eq. (2.23).

Using the argument principle to replace the sum we then get the Casimir energy of two semitransparent plates in a Dirichlet annulus, the immediate generalization of the Casimir energy (4.26) for a single plate,

$$\mathcal{E} = \frac{1}{8\pi^2 i} \int_0^\infty \kappa d\kappa \int_\gamma d\eta \left(\frac{\partial}{\partial\eta} \ln[K_{i\eta}(\kappa a)\tilde{I}_{i\eta}(\kappa b) - \tilde{I}_{i\eta}(\kappa a)K_{i\eta}(\kappa b)]\right)$$
$$\times \ln\left(1 - \frac{\lambda_1\lambda_2\cosh^2\eta(\pi - \alpha)}{(2\eta\sinh\eta\pi + \lambda_1\cosh\eta\pi)(2\eta\sinh\eta\pi + \lambda_2\cosh\eta\pi)}\right). \qquad (4.39)$$

A limiting case when $a, b \to \infty$, $b - a$ fixed, should be two perpendicular semitransparent planes, a distance d apart, sandwiched between Dirichlet planes, similar to the single plate situation treated in the subsection above. A similar formula should then be

$$\mathcal{E} = \frac{1}{8\pi^2 i} \int_0^\infty \kappa d\kappa \int_\gamma d\tilde{\eta} \left(\frac{\partial}{\partial\tilde{\eta}} \ln\left[\frac{\sin(\sqrt{\tilde{\eta}^2 - \kappa^2}(b - a))}{\sqrt{\tilde{\eta}^2 - \kappa^2}}\right]\right) \ln\left(1 - \frac{\tilde{\lambda}_1\tilde{\lambda}_2 e^{-2\tilde{\eta}d}}{(2\tilde{\eta} + \tilde{\lambda}_1)(2\tilde{\eta} + \tilde{\lambda}_2)}\right). \qquad (4.40)$$

As in the case of a single plate, this limiting form is immediately obtained from Eq. (4.39).

Finally, we verify that we obtain the expression (2.24) for the wedge geometry. To do this, we must include the modes exterior to the outer cylinder (with the wedge extended to infinity as in Fig. 1) and subtract the energy present if the outer cylinder were not present. This means that the radial dispersion function determining the azimuthal eigenvalues η becomes

$$\hat{R}_\eta(b; \kappa) = (K_{i\eta}(\kappa a)\tilde{I}_{i\eta}(\kappa b) - \tilde{I}_{i\eta}(\kappa a)K_{i\eta}(\kappa b))$$
$$\times \frac{K_{i\eta}(\kappa b)}{K_{i\eta}(\kappa a)}. \tag{4.41}$$

The extended annular energy is then given by Eq. (4.39) with $\tilde{R}_\eta(b; \kappa) \to \hat{R}_\eta(b; \kappa)$. We now can distort the contour γ to one lying along the imaginary axis as shown in Fig. 3, $i\eta \to \nu$ [because the second logarithm in Eq. (4.39) falls off exponentially fast for $\operatorname{Re}\eta > 0$], and then using the small argument expansion, for real ν,

$$K_\nu(x) \sim \frac{\Gamma(|\nu|)}{2}\left(\frac{x}{2}\right)^{-|\nu|},$$
$$\tilde{I}_\nu(x) \sim \frac{\sin|\nu|\pi}{\pi}\frac{\Gamma(|\nu|)}{2}\left(\frac{x}{2}\right)^{-|\nu|}, \qquad x \to 0. \tag{4.42}$$

This means for small a and real ν the first logarithm in Eq. (4.39) is $\ln I_\nu(\kappa b)K_\nu(\kappa b)$, which is just what was encountered in Eq. (2.17). We then fold the ν integral to encircle the positive real axis as in Fig. 8 and integrate by parts in κ and ν. In this way the form (2.16) is reproduced (with $D \to \hat{D}$), which leads to the final expression (2.24).

G. Numerical evaluation of the Casimir energy for two Dirichlet planes in an annulus

The Casimir energy in Eq. (4.37) is a quickly converging function so it should be easy to evaluate. However, it can be difficult to evaluate the η eigenvalues, which become functions of the wave number κ and a natural number m. We can get around this problem, again, by exploiting the argument principle in order to get a contour integral in the complex plane, as in Eq. (4.39). We cannot integrate along the real line because of the poles introduced when we use the argument principle, and unlike with the wedge we cannot open along the imaginary axis, because the integral then becomes divergent. So a simple choice is then to let the integration run along the angles of $\pi/4$ and $-\pi/4$ in the complex η plane. Identifying $R_\eta(b, \kappa)$ from Eq. (4.18), and writing $\operatorname{tr}g_\eta^{(1)}v_1 g_\eta^{(2)}v_2 = A(\eta)$, we have

$$\mathcal{E} = \frac{1}{4\pi^2}\int_0^\infty \kappa d\kappa \int_0^\infty d\nu\Bigg\{\frac{\operatorname{Re}R_{\sqrt{i}\nu}\partial_\nu\operatorname{Re}R_{\sqrt{i}\nu} + \operatorname{Im}R_{\sqrt{i}\nu}\partial_\nu\operatorname{Im}R_{\sqrt{i}\nu}}{|R_{\sqrt{i}\nu}|^2}\arctan\left(\frac{\operatorname{Im}A(\sqrt{i}\nu)}{1 - \operatorname{Re}A(\sqrt{i}\nu)}\right)$$
$$- \frac{\operatorname{Re}R_{\sqrt{i}\nu}\partial_\nu\operatorname{Im}R_{\sqrt{i}\nu} - \operatorname{Im}R_{\sqrt{i}\nu}\partial_\nu\operatorname{Re}R_{\sqrt{i}\nu}}{2|R_{\sqrt{i}\nu}|^2}\ln(1 - 2\operatorname{Re}A(\sqrt{i}\nu) + |A(\sqrt{i}\nu)|^2)\Bigg\}. \tag{4.43}$$

Here we have used the property that $R_{\eta^*} = R_\eta^*$, and $A(\eta^*) = A^*(\eta)$. The value of $R_{\sqrt{i}\nu}(b, \kappa)$ is obtained as a numerical solution to the differential equation. Using this technique we can obtain a numerical energy in about 1 cpu second. The results of this calculation are found in Fig. 10.

Again we would like to compare to known results, so Fig. 11 is a graph of the ratio of the energies of an annular piston to a rectangular piston of similar dimension. The rectangular piston is constructed so it has the same finite width $b - a$ as the annular piston, and the separation distance is the mean distance between the annular plates,

$$d = \frac{b + a}{2}2\sin\left(\frac{\alpha}{2}\right). \tag{4.44}$$

The results make a certain amount of physical sense. The energy of the annular piston is greater than that of the rectangular piston for small separation because the inner edge of the annular piston is closer, and will contribute more to the energy. However as the annular piston gets farther away, the other side of the piston will start to contribute and lower the overall energy. In addition we see that the small piston is much closer to the rectangular

piston for small separations than a larger piston, and in the plateau region for small separations, $E_{\text{ann}}/E_{\text{rect}} \approx 1.004$ for $b/a = 1.1$ vs $E_{\text{ann}}/E_{\text{rect}} \approx 1.23$ for $b/a = 2$. These numbers are quite closely reproduced by the ratio of the
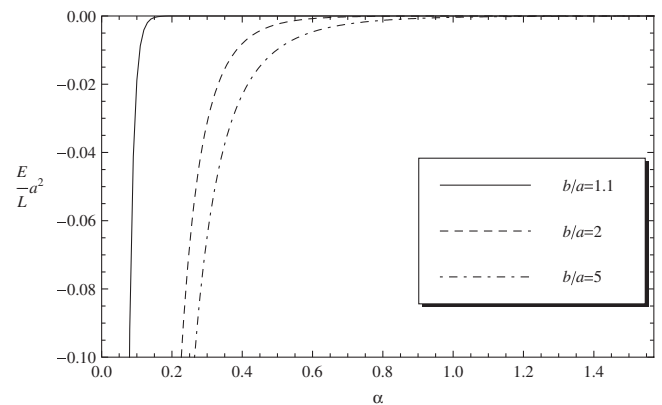

FIG. 10. This figure shows the energy per length vs the angle between Dirichlet plates. The energy is scaled by the inner radius a. The three lines represent three different ratios of inner to outer radius $\frac{b}{a} = 1.1$, $\frac{b}{a} = 2$, and $\frac{b}{a} = 5$.
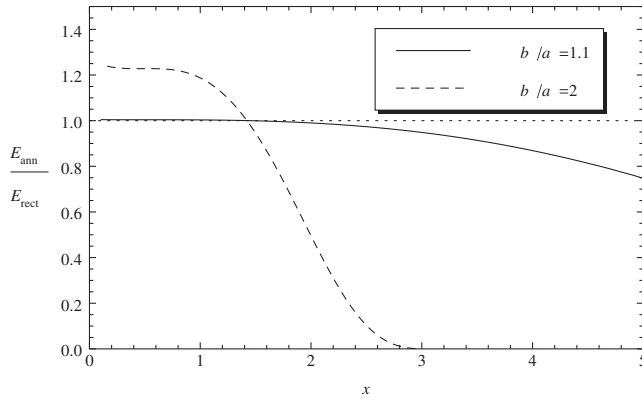
FIG. 11. This figure shows the ratio of the energies of an annular Dirichlet piston to a rectangular Dirichlet piston of similar dimension vs average separation distance between the plates. The variable x is the separation distance scaled by the finite size of the piston $b - a$, $x = d/(b - a)$. The two lines represent two ratios of inner to outer radius $\frac{b}{a} = 1.1$, and $\frac{b}{a} = 2$. For the latter case, only the region $\alpha \in [0, \pi]$ is shown.

proximity force approximate value of the energy for tilted plates to the energy for parallel plates (ignoring the side-walls) for small tilt angles,

$$\frac{\mathcal{E}_{\text{PFA}}}{\mathcal{E}_{\parallel}} = \frac{1}{16} \frac{b^2}{a^2}\left(1 + \frac{a}{b}\right)^4. \qquad (4.45)$$

V. THETA DEPENDENT POTENTIALS

Instead of considering, as usually done, spherically or cylindrically symmetric potentials, in this paper we have been examining potentials depending on the angles. In particular, in two dimensions, in order for separation of variables to work, we have been considering the operator

$$L = -\nabla^2 + \frac{1}{\rho^2} v(\theta)$$
$$= -\frac{\partial^2}{\partial \rho^2} - \frac{1}{\rho} \frac{\partial}{\partial \rho} - \frac{1}{\rho^2} \frac{\partial^2}{\partial \theta^2} + \frac{1}{\rho^2} v(\theta), \qquad (5.1)$$

with $v(\theta)$ given in Eq. (2.1). The advantage of this potential is that a closed form for the secular equation can be given [see Eq. (2.11)]. But what can be said for other potentials $v(\theta)$? The relevant equations for the two-dimensional Green's function are still Eqs. (2.5), (2.6), (2.7), (2.8), (2.9), (2.10a), and (2.10b). In particular, for the angular eigenfunctions we still have

$$0 = \Theta''(\theta) + (\nu^2 - v(\theta))\Theta(\theta), \qquad (5.2)$$

where ν is the separation constant. The separation constant is determined from the boundary condition in θ. For $v(\theta)$ being a smooth potential, one imposes periodic boundary conditions, and this is what we concentrate on for concreteness.

Note that the only information from Eq. (5.2) that enters Eq. (2.9) for the radial reduced Green's function is the separation constant ν. From Eq. (5.2) its square can be considered the eigenvalue of

$$L_\theta = -\frac{\partial^2}{\partial \theta^2} + v(\theta) \qquad (5.3)$$

with periodic boundary conditions. For a nontrivial potential $v(\theta)$ no explicit form of ν will be known. But also in general a transcendental equation determining the eigenvalues can be obtained; we follow Ref. [48]. In order to formulate this equation let $H(\theta)$ be the fundamental matrix of Eq. (5.2). That is, let $u_\nu^{(1)}(\theta)$ and $u_\nu^{(2)}(\theta)$ be two linearly independent solutions of Eq. (5.2). With $w_\nu^{(i)}(\theta) = du_\nu^{(i)}(\theta)/d\theta$, the fundamental matrix is

$$H(\theta) = \begin{pmatrix} u_\nu^{(1)}(\theta) & u_\nu^{(2)}(\theta) \\ w_\nu^{(1)}(\theta) & w_\nu^{(2)}(\theta) \end{pmatrix}, \qquad (5.4)$$

where we choose the normalizations such that $H(0) = 1_{2\times 2}$. With these definitions and normalizations, the equation determining the eigenvalues reads

$$0 = D(\nu)$$
$$= (1 - u_\nu^{(1)}(2\pi))(1 - w_\nu^{(2)}(2\pi)) - u_\nu^{(2)}(2\pi)w_\nu^{(1)}(2\pi). \qquad (5.5)$$

The solutions to this equation have to be used in Eq. (2.9). The Casimir energy expressions (2.16) and (2.17) then remain valid, once the appropriate radial reduced Green's function is used and $D(\nu)$ given in Eq. (5.5) is substituted. Once $v(\theta)$ is specified this allows, in principle, for a numerical evaluation of the Casimir energy when suitable subtractions are performed.

APPENDIX A: AN INTEGRAL THEOREM

It may be useful to see explicitly how the trace of the subtracted reduced Green's function turns into a derivative of a logarithm, as in Eq. (2.17). Consider a Green's function $g_\kappa(x, x')$ for a one-dimensional problem described by

the differential equation

$$\left[-\frac{d}{dx}p(x)\frac{d}{dx} - \kappa^2 r(x) + q(x) + p(x)V(x)\right]g_\kappa(x, x')$$
$$= \delta(x - x'), \tag{A1}$$

where V is a δ-function potential,

$$V(x) = \lambda\delta(x - c). \tag{A2}$$

The problem is defined on the interval $a < c < b$, where at the boundaries g_κ satisfies Dirichlet boundary conditions,

$$g_\kappa(a, x') = g_\kappa(b, x') = 0. \tag{A3}$$

If the potential $V = 0$, let the corresponding Green's function be denoted by $g_\kappa^{(0)}$.

Let us solve this problem in terms of two independent solutions of the homogeneous equation

$$\left[-\frac{d}{dx}p(x)\frac{d}{dx} - \kappa^2 r(x) + q(x)\right]u_\kappa(x) = 0. \tag{A4}$$

Let A_κ be such a solution that vanishes at the left boundary, $A_\kappa(a) = 0$, and B_κ be an independent solution that vanishes at the right boundary, $B_\kappa(b) = 0$, and let them be normalized so that the Wronskian is

$$W[A_\kappa, B_\kappa](x) \equiv A_\kappa(x)B_\kappa'(x) - B_\kappa(x)A_\kappa'(x) = -\frac{1}{p(x)}. \tag{A5}$$

Then the "free" Green's function is

$$g_\kappa^{(0)}(x, x') = A_\kappa(x_<)B_\kappa(x_>), \tag{A6}$$

and the full Green's function has the form

$$g_\kappa(x, x') = g_\kappa^{(0)}(x, x') + \begin{cases} \alpha A_\kappa(x)A_\kappa(x'), & a < x, x' < c, \\ \beta B_\kappa(x)B_\kappa(x'), & c < x, x' < b. \end{cases} \tag{A7}$$

Now, it is easy to prove that

$$\alpha = \frac{\lambda B_\kappa^2(c)}{\lambda A_\kappa(c)B_\kappa(c) + 1}, \qquad \beta = \frac{\lambda A_\kappa^2(c)}{\lambda A_\kappa(c)B_\kappa(c) + 1}. \tag{A8}$$

It is immediate that any two solutions of the differential equation (A4) u_κ and w_κ satisfy

$$\frac{\partial}{\partial x}\left[p(x)\left(\frac{\partial}{\partial x}u_\kappa(x)\frac{\partial}{\partial \kappa}w_\kappa(x) - u_\kappa(x)\frac{\partial}{\partial \kappa}\frac{\partial}{\partial x}w_\kappa(x)\right)\right] = 2\kappa r(x)u_\kappa(x)w_\kappa(x), \tag{A9}$$

and therefore the following indefinite integral follows:

$$\int dxr(x)u_\kappa^2(x) = \frac{p(x)}{2\kappa}u_\kappa(x)u_\kappa'(x)\frac{\partial}{\partial \kappa}\ln\frac{u_\kappa(x)}{u_\kappa'(x)}, \tag{A10}$$

where $u_\kappa'(x) \equiv \frac{\partial}{\partial x}u_\kappa(x)$.

Now we can evaluate the trace of the interaction part of the Green's function,

$$\mathrm{tr}(g - g^{(0)}) \equiv \int_a^b dxr(x)[g(x, x) - g^{(0)}(x, x)]$$
$$= \frac{\lambda}{\lambda A_\kappa(c)B_\kappa(c) + 1}\left[B_\kappa^2(c)\int_a^c dxr(x)A_\kappa^2(x) + A_\kappa^2(c)\int_c^b dxr(x)B_\kappa^2(x)\right]$$
$$= -\frac{p(c)}{2\kappa}\frac{\lambda A_\kappa^2(c)B_\kappa^2(c)}{\lambda A_\kappa(c)B_\kappa(c) + 1}\left[\frac{A_\kappa'(c)}{A_\kappa(c)}\frac{d}{d\kappa}\ln\frac{A_\kappa'(c)}{A_\kappa(c)} - \frac{B_\kappa'(c)}{B_\kappa(c)}\frac{d}{d\kappa}\ln\frac{B_\kappa'(c)}{B_\kappa(c)}\right]$$
$$= \frac{d}{d\kappa^2}\ln[1 + \lambda A_\kappa(c)B_\kappa(c)] = \frac{d}{d\kappa^2}\ln[1 + \lambda g^{(0)}(c, c)]. \tag{A11}$$

This is the expected expression. As shown in Sec. IV E, this is just the expected multiple-scattering result. In the Dirichlet limit $\lambda \to \infty$, this agrees with the Bessel function result (2.17), where $p(x) = r(x) = x$; although in that case the boundary condition is not Dirichlet at the origin, $p(0) = 0$.

APPENDIX B: MODIFIED BESSEL FUNCTIONS OF PURE IMAGINARY ORDER

In this work we encountered the following differential equation,

$$\left(x\frac{\partial}{\partial x}x\frac{\partial}{\partial x} - x^2 + \eta^2\right)\psi(x) = 0, \tag{B1}$$

which is the modified Bessel equation, with the wrong sign

for the order parameter η^2. The solutions are then obviously modified Bessel functions of imaginary order. So we might choose as the independent pair of solutions the modified Bessel function of the first kind, of positive and negative pure imaginary order $I_{i\eta}(x)$ and $I_{-i\eta}(x)$. However the $I_{i\eta}$'s are not numerically satisfactory functions; their values for real x are complex, and the phase is x dependent. A standard pair of functions can be defined as

$$K_\nu(x) = \frac{\pi}{2\sin\nu\pi}(I_{-\nu}(x) - I_\nu(x)), \tag{B2a}$$

$$L_\nu(x) = \frac{i\pi}{2\sin\nu\pi}(I_\nu(x) + I_{-\nu}(x)). \tag{B2b}$$

The $K_\nu(x)$ is the standard modified Bessel function of the second kind, also called the Macdonald function. Both

$K_{i\eta}(x)$ and $L_{i\eta}(x)$ are real for real values of η and x. For a fixed η, both K and L oscillate with relatively constant amplitude for $x < \eta$, and they die or grow exponentially for $x > \eta$, respectively. The limiting behaviors are given in this appendix; see Refs. [45,46]. Although this definition of L_ν is convenient in Sec. II, for the considerations of Sec. IV, the $\sin\nu\pi$ in Eq. (B2b) introduces spurious singularities, and it is more convenient there to simply use

$$\tilde{I}_\nu(x) = \frac{1}{2}(I_\nu(x) + I_{-\nu}(x)) = \frac{\sin\nu\pi}{i\pi}L_\nu(x), \qquad \text{(B3)}$$

also called L_ν in Ref. [38]. In the following we will give the behaviors of $K_{i\eta}$ and $\tilde{I}_{i\eta}$.

1. Small argument

For fixed $\eta > 0$, in the limit as $x \to 0^+$,

$$K_{i\eta}(x) = -\left(\frac{\pi}{\eta\sinh\eta\pi}\right)^{1/2}\left[\sin\left(\eta\ln\frac{x}{2} - \phi_\eta\right) + \mathcal{O}(x^2)\right],$$
$$\text{(B4a)}$$

$$\tilde{I}_{i\eta}(x) = \left(\frac{\sinh\eta\pi}{\eta\pi}\right)^{1/2}\left[\cos\left(\eta\ln\frac{x}{2} - \phi_\eta\right) + \mathcal{O}(x^2)\right],$$
$$\text{(B4b)}$$

where ϕ_η is given by

$$\phi_\eta = \arg[\Gamma(1 + i\eta)]. \qquad \text{(B5)}$$

2. Large argument

For fixed $\eta > 0$ and large argument $|x| \to \infty$ we have

$$K_{i\eta}(x) = \left(\frac{\pi}{2x}\right)^{1/2}e^{-x}[1 + \mathcal{O}(x^{-1})], \qquad |\arg x| \le \frac{3\pi}{2} - \delta,$$
$$\text{(B6a)}$$

$$\tilde{I}_{i\eta}(x) = \left(\frac{1}{2\pi x}\right)^{1/2}e^x[1 + \mathcal{O}(x^{-1})], \qquad |\arg x| \le \frac{\pi}{2} - \delta,$$
$$\text{(B6b)}$$

for arbitrary $\delta > 0$.

3. Uniform asymptotic expansion

The uniform asymptotic expansions are for both large order and argument. For fixed $z > 0$ we have for the leading behavior

$$K_{i\eta}(\eta z) \sim \frac{\pi e^{-\eta\pi/2}}{\eta^{1/3}}\left(\frac{4\zeta}{1 - z^2}\right)^{1/4}\text{Ai}(-\eta^{2/3}\zeta), \qquad \text{(B7a)}$$

$$\tilde{I}_{i\eta}(\eta z) \sim \frac{e^{\eta\pi/2}}{2\pi\eta^{1/3}}\left(\frac{4\zeta}{1 - z^2}\right)^{1/4}\text{Bi}(-\eta^{2/3}\zeta), \qquad \text{(B7b)}$$

where the $\text{Ai}(x)$ and $\text{Bi}(x)$ are the Airy functions of the first and second kinds, respectively, and ζ is given by the relation

$$\frac{2}{3}\zeta^{3/2} = f(z), \qquad f(z) = \ln\left(\frac{1 + \sqrt{1 - z^2}}{z}\right) - \sqrt{1 - z^2}.$$
$$\text{(B8)}$$

For $z < 1$ we can use the behavior of the Airy functions for large negative argument to simplify the expressions,

$$K_{i\eta}(\eta z) \sim \sqrt{\frac{2\pi}{\eta}}\frac{e^{-\eta\pi/2}}{(1 - z^2)^{1/4}}\cos\left(\eta f(z) - \frac{\pi}{4}\right), \qquad \text{(B9a)}$$

$$\tilde{I}_{i\eta}(\eta z) \sim -\sqrt{\frac{1}{2\pi\eta}}\frac{e^{\eta\pi/2}}{(1 - z^2)^{1/4}}\sin\left(\eta f(z) - \frac{\pi}{4}\right). \qquad \text{(B9b)}$$

If we choose the branch cut for Eq. (B8) such that ζ is a continuous real function of z, then for $z > 1$ we can simplify the expressions to read

$$K_{i\eta}(\eta z) \sim \sqrt{\frac{\pi}{2\eta}}\frac{e^{-\eta\pi/2}}{(z^2 - 1)^{1/4}}e^{-\eta g(z)}, \qquad \text{(B10a)}$$

$$\tilde{I}_{i\eta}(\eta z) \sim \sqrt{\frac{1}{2\pi\eta}}\frac{e^{\eta\pi/2}}{(z^2 - 1)^{1/4}}e^{\eta g(z)}, \qquad \text{(B10b)}$$

where $g(z)$ is the natural extension of $f(z)$

$$g(z) = -\text{arcsec}\,z + \sqrt{z^2 - 1}. \qquad \text{(B11)}$$

[1] H. B. G. Casimir, Proc. K. Ned. Akad. Wet. **51**, 793 (1948).

[2] K. A. Milton, *The Casimir Effect: Physical Manifestations of the Zero-Point Energy* (World Scientific, Singapore, 2001).

[3] K. A. Milton, J. Phys. A **37**, R209 (2004).

[4] S. K. Lamoreaux, Rep. Prog. Phys. **68**, 201 (2005).

[5] S. Y. Buhmann and D.-G. Welsch, Prog. Quantum Electron. **31**, 51 (2007).

[6] M. Bordag, G. L. Klimchitskaya, U. Mohideen, and V. M. Mostepanenko, *Advances in the Casimir Effect* (Oxford University Press, Oxford, 2009).

[7] L. L. DeRaad, Jr. and K. A. Milton, Ann. Phys. (N.Y.) **136**, 229 (1981).

[8] I. Brevik and G. H. Nyland, Ann. Phys. (N.Y.) **230**, 321 (1994).

[9] P. Gosdzinsky and A. Romeo, Phys. Lett. B **441**, 265 (1998).

[10] K. A. Milton, A. V. Nesterenko, and V. V. Nesterenko, Phys. Rev. D **59**, 105009 (1999).

[11] G. Lambiase, V. V. Nesterenko, and M. Bordag, J. Math. Phys. (N.Y.) **40**, 6254 (1999).

[12] I. Cavero-Peláez and K. A. Milton, Ann. Phys. (N.Y.) **320**, 108 (2005); J. Phys. A **39**, 6225 (2006).

[13] A. Romeo and K. A. Milton, Phys. Lett. B **621**, 309 (2005); J. Phys. A **39**, 6703 (2006).

[14] I. Brevik and A. Romeo, Phys. Scr. **76**, 48 (2007).

[15] I. Cavero-Peláez, K. A. Milton, and K. Kirsten, J. Phys. A **40**, 3607 (2007).

[16] J. S. Dowker and G. Kennedy, J. Phys. A **11**, 895 (1978).

[17] D. Deutsch and P. Candelas, Phys. Rev. D **20**, 3063 (1979).

[18] I. Brevik and M. Lygren, Ann. Phys. (N.Y.) **251**, 157 (1996).

[19] I. Brevik, M. Lygren, and V. Marachevsky, Ann. Phys. (N.Y.) **267**, 134 (1998).

[20] I. Brevik and K. Pettersen, Ann. Phys. (N.Y.) **291**, 267 (2001).

[21] V. V. Nesterenko, G. Lambiase, and G. Scarpetta, Ann. Phys. (N.Y.) **298**, 403 (2002).

[22] H. Razmi and S. M. Modarresi, Int. J. Theor. Phys. **44**, 229 (2005).

[23] V. M. Mostepanenko and N. N. Trunov, *The Casimir Effect and Its Applications* (Oxford University Press, Oxford, 1997).

[24] V. V. Nesterenko, G. Lambiase, and G. Scarpetta, J. Math. Phys. (N.Y.) **42**, 1974 (2001).

[25] V. V. Nesterenko, I. G. Pirozhenko, and J. Dittrich, Classical Quantum Gravity **20**, 431 (2003).

[26] A. H. Rezaeian and A. A. Saharian, Classical Quantum Gravity **19**, 3625 (2002).

[27] A. A. Saharian, Eur. Phys. J. C **52**, 721 (2007).

[28] A. A. Saharian, in *The Casimir Effect and Cosmology: A Volume in Honour of Professor Iver H. Brevik on the Occasion of His 70th Birthday*, edited by S. Odintsov *et al.* (Tomsk State Pedagogical University Press, Tomsk, Russia, 2008), p. 87.

[29] A. A. Saharian and A. S. Tarloyan, J. Phys. A **38**, 8763 (2005).

[30] A. A. Saharian and A. S. Tarloyan, Ann. Phys. (N.Y.) **323**, 1588 (2008).

[31] G. Barton, Proc. R. Soc. London **410**, 175 (1987).

[32] S. C. Skipsey, G. Juzeliūnas, M. Al-Amri, and M. Babiker, Opt. Commun. **254**, 262 (2005).

[33] S. C. Skipsey, M. Al-Amri, M. Babiker, and G. Juzeliūnas, Phys. Rev. A **73**, 011803(R) (2006).

[34] T. N. C. Mendes, F. S. S. Rosa, A. Tenório, and C. Farina, J. Phys. A **41**, 164 029 (2008).

[35] F. S. S. Rosa, T. N. C. Mendes, A. Tenório, and C. Farina, Phys. Rev. A **78**, 012105 (2008).

[36] C. I. Sukenik, M. G. Boshier, D. Cho, V. Sandoghdar, and E. A. Hinds, Phys. Rev. Lett. **70**, 560 (1993).

[37] I. Brevik, S. Å. Ellingsen, and K. A. Milton, Phys. Rev. E **79**, 041120 (2009).

[38] S. Å. Ellingsen, I. Brevik, and K. A. Milton, Phys. Rev. E **80**, 021125 (2009).

[39] N. G. van Kampen, B. R. A. Nijboer, and K. Schram, Phys. Lett. **26A**, 307 (1968).

[40] M. Bordag, E. Elizalde, and K. Kirsten, J. Math. Phys. (N.Y.) **37**, 895 (1996).

[41] V. A. Parsegian, *Van Der Waals Forces* (Cambridge University Press, Cambridge, 2006), Sec. L3.3.

[42] I. Brevik, B. Jensen, and K. A. Milton, Phys. Rev. D **64**, 088701 (2001).

[43] V. V. Nesterenko, J. Phys. A **39**, 6609 (2006).

[44] V. V. Nesterenko, J. Phys. A **41**, 164 005 (2008).

[45] T. M. Dunster, SIAM J. Math. Anal. **21**, 995 (1990).

[46] F. W. J. Olver, *Asymptotics and Special Functions* (Academic Press, New York, 1974), Chaps. 10–12.

[47] K. A. Milton and J. Wagner, J. Phys. A **41**, 155 402 (2008).

[48] K. Kirsten and A. J. McKane, J. Phys. A **37**, 4649 (2004).